LASER & PHOTONICS REVIEWS
www.lpr-journal.org

Pulsed Quantum Excitation

Juan Camilo López Carreño

A two-level system (2LS) is the most fundamental building block of matter. Its response to classical light is well known, as it converts pulses of coherent light into antibunched emission. Recently, theoretical proposals have predicted that it is advantageous to illuminate two-level systems with Quantum Light; i.e., the light emitted from a quantum system. However, those proposals are done considering continuous excitation of the source of light. Here, the field is advanced by changing the paradigm of excitation: we use the emission of a 2LS, itself driven by a laser pulse, to excite another 2LS. Thus, a thorough analysis of Resonance Fluorescence under pulsed quantum excitation is presented, showing that, in particular, the emission from a 2LS driven with quantum light is more antibunched and more indistinguishable than if it were driven with classical light. The results reinforce the claim of the advantage of the excitation with quantum light, provide support to the recent experimental observations, and can be used as a road-map for the future of light-matter interaction research.

1. Introduction

Excitation with Quantum Light, understood as using the light emitted from a quantum system as a resource to drive optical targets, is an idea as old as the field of Quantum Optics.[1–3] The advent of reliable sources of antibunched[4] and squeezed light[5,6] motivated the development of a theoretical framework to describe adequately such an excitation. Thus, in 1993 Gardiner[7] and Carmichael[8] independently introduced the formalism that we now know as the "theory of cascaded systems", which is based on the input–output theory of quantum optics. Since its development, this theory has been used to explore fundamental topics, including chirality in non-hermitian systems,[9,10] the shaping of flying qubits,[11] and quantum steering;[12] but also to implement practical applications, such as feeding forward information into quantum reservoir networks.[13–15]

From the point of view of the source of quantum light, the most fundamental system that one can consider is Resonance Fluorescence. Described as two energy levels that become dressed as they interact with a strong coherent field, it yields the celebrated *Mollow triplet* spectrum.[16] Such a system has a rich underlying structure,[17] whereby the photons emitted from various frequency regions display a large gamut of correlations.[18,19] Using this variety of photon correlations to excite fermionic[20] and bosonic fields[21] strengthens their quantum features (for example, leading to better antibunching in the final emission) and lets them access quantum states that are unreachable when they are illuminated with classical light. Notably, the Mollow triplet can be used to perform an unprecedented quantum spectroscopy technique, whereby the internal structure of the target of the excitation is probed with only two photons.[22]

A natural advancement in the analysis of Resonance Fluorescence was to upgrade the continuous-wave driving, and consider pulsed excitation instead. Under such a regime, the emission spectrum consists of multiple peaks,[23–28] whose linewidths and intensities depend on the strength and duration of the pulse.[29,30] The appearance of the multiple-peaked structure has recently been observed in semiconductor[31] and superconducting quantum dots,[32] as well as in cavity-QED systems.[33] Importantly, the spectral correlations of the emitted photons are still present under this regime of excitation.[34,35]

In this Article, we go beyond the analysis of pulsed Resonance Fluorescence, and instead exploit its emission as a source of quantum light. Using a two-level system (2LS) as the optical target of the excitation, we present here a direct comparison between classical and quantum pulsed excitation, and showcase the benefits of the latter for the implementation of quantum technologies. The choice of source and target considered in this Article allows us to provide an in-depth analysis of a recent experimental observation of the excitation of a quantum dot with a pulse of quantum light.[36] Thus, the rest of the manuscript is organised as follows. Section 2 provides the theoretical tools used to describe the excitation of the source 2LS with a laser pulse (cf. **Figure 1**), and the subsequent cascade of quantum light directed towards the target 2LS. Next, in sections 3—5 we compare the single-particle observable of the emission, considering the dynamic Rabi oscillations, the occupation and the time-integrated emission spectrum. Later, in section 6 we discuss the two-particle observables. There, we present evidence of stimulated emission at the single-particle level and show that quantum excitation yields an enhancement

J. C. López Carreño
Center for Theoretical Physics
Polish Academy of Sciences
Aleja Lotników 32/46, 02-668 Warsaw, Poland
E-mail: juclopezca@cft.edu.pl

J. C. López Carreño
Institute of Experimental Physics, Faculty of Physics
University of Warsaw
ul. Pasteura 5, 02-093 Warsaw, Poland

DOI: 10.1002/lpor.202501375

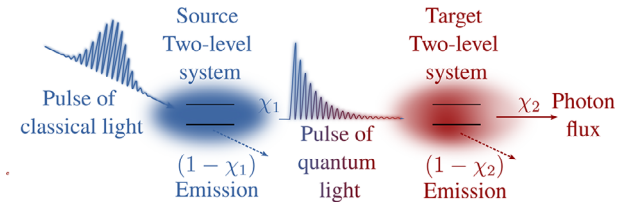

Figure 1. Sketch of the cascaded excitation. A classical pulse of light (blue line) is used to excite a two-level system, here depicted as a glowing halo around a pair of energy levels. A fraction χ_1 of the emission from the source 2LS becomes the source of quantum excitation of the target 2LS (line with blue-to-red gradient coloring). After the interaction between the target 2LS and the quantum excitation we can collect two fields: namely, a fraction χ_2 corresponding to the photon flux of the entire system, and the remaining fraction $(1-\chi_2)$ associated with the individual emission from the target 2LS.

in the antibunching and the indistinguishability of the emitted photons. Finally, in section 7, we conclude and present the perspectives of our work.

2. Theoretical Description

The first stage of the excitation, used to power the source of quantum light, is done with laser pulse and it is modelled through the Hamiltonian (we take $\hbar = 1$ along the manuscript)

$$H_\sigma(t) = (\omega_\sigma - \omega_L)\sigma^\dagger\sigma + \frac{\Omega(t)}{2}(\sigma + \sigma^\dagger) \tag{1}$$

where σ is the annihilation operator associated to the 2LS (and which follows the pseudo-spin algebra). Here, we have also defined the natural frequency of the 2LS ω_σ, the frequency of the pulse laser ω_L, and the time-dependent intensity of the pulse $\Omega(t)$. The dissipative character of the system is taken into account by upgrading the description to a master equation

$$\partial_t\rho = i[\rho, H_\sigma(t)] + \frac{\gamma_\sigma}{2}\mathcal{L}_\sigma(\rho) \tag{2}$$

where $H_\sigma(t)$ is the Hamiltonian introduced in Equation (1), $\mathcal{L}_c(\rho) = (2c\rho c^\dagger - c^\dagger c\rho - \rho c^\dagger c)$, and γ_σ is the decay rate of the 2LS. Commonly, the laser pulse has a Gaussian profile, given by

$$\Omega(t) = \frac{A}{\sqrt{2\pi\nu^2}}\exp\left[-\frac{(t-t_0)^2}{2\nu^2}\right] \tag{3}$$

which corresponds to a pulse with integrated area A, centered at time t_0 and with variance ν^2. The latter is related to the full width at half maximum (FWHM) through the relation $\mathcal{W} = 2\sqrt{2\log 2}\nu$; and along this manuscript we will refer to $\mathcal{W}$ as the length of the pulse.

In the second stage of the excitation, the emission from the classically excited 2LS is directed toward the second 2LS which, as a consequence, is driven with a quantum field. (The details of the experimental setup to realise such a quantum excitation can be found in the Supporting Information of Ref. [36]. Note that in that particular experiment the quantum emitter was embedded in a microcavity. However, the role of the latter was purely technical; namely, to enhance the efficiency of excitation of the emitter, and did not have any other effect in the dynamics of the quantum emitter. Therefore, our description can safely omit the microcavity and still reproduce the experimental observations.) From a theoretical point of view, such an excitation is a perfect example of the dynamics that inspired the theory of cascaded systems.[7,8] Therefore, the master equation that describes the full system, including the quantum excitation, and which reproduces the experimental results of Ref. [36], becomes

$$\begin{aligned}\partial_t\rho = {} & i\left[\rho, H_\sigma(t) + H_\xi\right] + \frac{\gamma_\sigma}{2}\mathcal{L}_\sigma(\rho) + \frac{\gamma_\xi}{2}\mathcal{L}_\xi(\rho) \\ & - \sqrt{\chi_1\chi_2\gamma_\sigma\gamma_\xi}\left\{\left[\xi^\dagger, \sigma\rho\right] + \left[\rho\sigma^\dagger, \xi\right]\right\} .\end{aligned} \tag{4}$$

Here, ξ is the annihilation operator of the target 2LS, which decays with rate γ_ξ. The Hamiltonian $H_\xi = (\omega_\xi - \omega_L)\xi^\dagger\xi$ describes the free energy of the target 2LS, which also showcases the detuning between the natural frequency of the target 2LS ω_ξ and the laser driving the source 2LS. The excitation with quantum light is modelled in Equation (4) through the term in the second line. It provides an unidirectional coupling between the source and target, in such a way that the dynamics of the former is not affected by the presence of the latter. Namely, there is no back-action from the target to the source of quantum light. Here, it is important to note that when the emitters are far enough from each other, so that their dipole interaction can be omitted, but closer than the coherence length of their emission, one could enter regimes of "delayed feedback".[37,38] In such cases, the dynamics of the system becomes non-Markovian,[39–41] which has been investigated in the context, e.g., of the variation of the rate of spontaneous emission of individual atoms,[42–46] bound states in the continuum[47–49] and entanglement generation with emitters coupled to waveguides.[50–52] While these phenomena are interesting on their own merits, in this manuscript we remain in the regime where the target 2LS does not give any feedback to the source 2LS.

Turning back to our master equation, the parameters χ_1 and χ_2 that appear in the coefficient of this coupling are related to the degree to which each of the 2LS is able to couple to the other one. This is more easily seen when the master Equation (4) is rearranged in the Lindblad form, and we interpret the result in terms of quantum jump operators.[53] (See, e.g., the Supporting Information of Ref. [54] for the details of the general transformation, and the Supporting Information of this manuscript for a detailed derivation of the equations presented here.) Then, we find that the emission from the 2LSs is ruled by the operators

$$J_\sigma = \sqrt{(1-\chi_1)\gamma_\sigma}\sigma \qquad \text{and} \qquad J_\xi = \sqrt{(1-\chi_2)\gamma_\xi}\xi \tag{5}$$

In practice, this means that, e.g., the intensity of the emission from the source 2LS is decreased by a factor $(1-\chi_1)$, because the rest of the energy is used to excite the other 2LS. Finally, there is a third Lindblad term that mixes the operators from the two 2LS. Namely, J_ϕ defined as

$$J_\phi = \sqrt{\chi_1\gamma_\sigma}\sigma + \sqrt{\chi_2\gamma_\xi}\xi \tag{6}$$

which, is commonly referred to as the photon flux[55,56] and, as we shall see in the following sections, induces a quantum interference that provides a mechanism to stimulated emission of the target 2LS.

From the decomposition above we can clearly see the interplay between the strength of the cascaded coupling $\sqrt{\chi_1\chi_2\gamma_\sigma\gamma_\xi}$ and the jump operators of the system. Namely, neither χ_1 nor χ_2 can be zero, because it would mean that the two 2LS are not coupled. On the other hand, if they are set to 1, then the jump operators in Equation (5) are zero. In principle, this is not a problem. However, it implies that one cannot observe the emission from the 2LSs "on their own", and instead one can only see the collective emission through the photon flux. Given that we can collect the information from the source 2LS independently (that is, without the cascaded coupling, because the presence, or absence, of the optical target does not affect the dynamics of the source 2LS), and that for the target 2LS using $0 \leq \chi_1 < 1$ is equivalent to using a weaker source, we will consider the case $\chi_1 = 1$. In our particular case, letting $\chi_1 = 1$ means that the laser light is completely removed from the observables of the 2LSs. Therefore, unlike the experimental case, our theoretical description does not require any further technique to prevent contamination from the source of classical excitation. On the other side, for the target 2LS we want to keep the ability to observe the field on its own, as well as on the photon flux of the system. Thus, as a compromise between the two dissipative channels, in the main text we will set $\chi_2 = 1/2$. However, in the Supporting Information, we show how our results change for other values of χ_2. In practice, χ_1 is the fraction of the emission of the source 2LS that does not carry scattering or photons from the driving laser. Namely, the fraction of emission that originates only from the luminescence of the 2LS. Similarly, the emission from the target 2LS can also be split into a fraction $(1-\chi_2)$ containing only its luminescence, and the remaining fraction χ_2 that consists of the photon flux of the entire system; namely, part of the luminescence of the target 2LS together with scattered photons from the source of excitation. In the following, therefore, we will show the behaviour of the luminescence of a 2LS driven with classical light (labeled as Source 2LS), the luminescence of a 2LS driven with quantum light (labeled as Target 2LS), and the field observed experimentally in Ref. [36], namely, the superposition of the luminescence of the target 2LS and the (quantum) excitation field (labeled as Photon flux).

3. Pulsed Rabi Oscillations

The response of the classically excited 2LS as a function of the area of the laser pulse is well known.[57,58] Namely, for short-enough pulses, once the 2LS has interacted with the entirety of the pulse, the probability of finding the 2LS on its excited state is given by

$$P_e = \sin^2(A/2) \tag{7}$$

where A is the integrated area of the pulse. This is known as the area theorem.

Thus, one expects Rabi oscillations with unit visibility as a function of the area of the pulse, as shown in the dashed line in **Figure** 2a. However, although Equation (7) is a good approximation for very short pulses, even for $\mathcal{W}\gamma_\sigma = 0.1$ we find a deviation from the perfect oscillatory behaviour,[59–61] as shown as a solid line Figure 2a. In fact, as the length of the pulse is increased, the oscillations become increasingly damped, up to the point in which the intensity of the light increases monotonically as a function of the pulse area. Such a behaviour is illustrated in Figure 2b, where we show the integrated intensity as a function of the pulse area. Namely, the panels in the lower row display

$$I_c = \int_0^\infty \langle c^\dagger c\rangle(t)\, dt \tag{8}$$

for $c = \{\sigma, \xi, J_\phi\}$, respectively. The upper limit of integration is taken so that the entire response of the field is captured. There we can also see that, although for short pulses the position of the minima and maxima of the oscillations are given by odd- and even-π pulses, respectively, as the length of the pulses increases, these positions drift away. Therefore, the length of the pulse, together with the decay of the emitter and its coupling to phonons,[58] is yet another cause of the shift of the maxima of the Rabi oscillations.

Further, we can quantify the visibility the oscillations through the ratio

$$\mathcal{V} = \frac{M_\pi - m_{2\pi}}{M_\pi + m_{2\pi}} \tag{9}$$

where M_π is the maximum of the intensity around π-pulses, and $m_{2\pi}$ is the minimum of the intensity around 2π-pulses. For the 2LS driven classically, the visibility of the oscillations is shown as a dashed line in Figure 2c, which displays and exponential decay as a function of the pulse length; namely, the visibility of the oscillations can be fitted as

$$\mathcal{V} \propto \exp(-\beta\mathcal{W}\gamma_\sigma) \tag{10}$$

where β is the extinction coefficient, which for the source 2LS we fitted to $\beta = 1.87$. Further, the dashed black line in Figure 2c shows that the oscillations are completely extinguished for pulses of length $\mathcal{W}\gamma_\sigma \geq 2$.

We now turn to the Rabi oscillations of the target 2LS and the photon flux, described with the operators ξ and J_ϕ, introduced in Equations (4) and (6), respectively. The oscillations of the target 2LS are shown in Figure 2e, where we find that they are much more robust to the length of the classical pulse, remaining visible for pulses of length up to four times the lifetime of the 2LS, as shown in the blue shaded region of Figure 2c. There, the upper two lines show the visibility for $\chi_2 \to 0$ (black) and $\chi_2 \to 1$ (blue), and the color gradient indicates the variation of the parameter of the cascaded coupling χ_2. Notably, as shown in Figure 2c,d, the Rabi oscillations of the target 2LS are always more visible and decay more slowly than those of the source 2LS. Conversely, for the photon flux, whose oscillations are shown in Figure 2f, we find that their oscillations are, at best, as visible as the oscillations of the source 2LS. The lower two lines in Figure 2c show the visibility for $\chi_2 \to 0$ (dashed black, which corresponds to the visibility of the source 2LS) and $\chi_2 \to 1/2$ (red). Note that for the photon flux, as $\chi_2 > 1/2$, the visibility of the oscillations increases again. Finally, we can also fit the visibility lines with Equation (10), thus

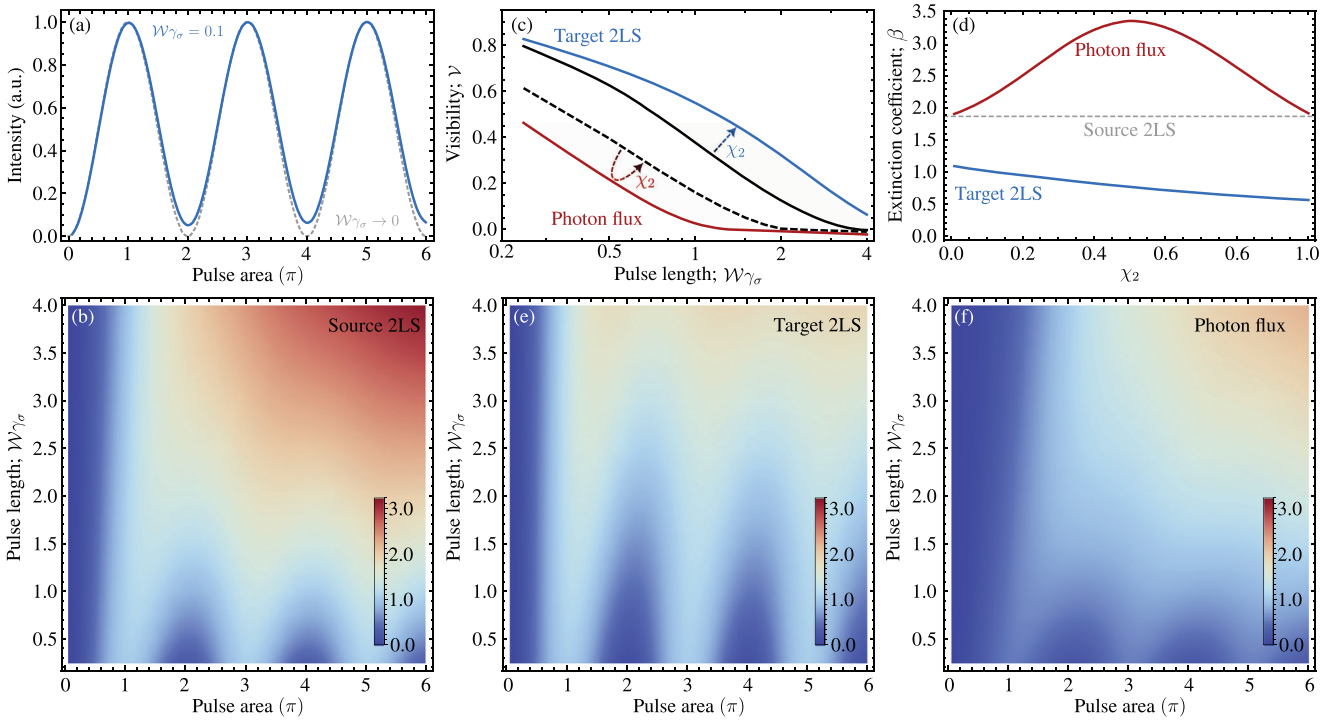

Figure 2. Pulsed Rabi oscillations. a) Intensity of the emission from a 2LS pulsed with a laser with vanishing (dashed line) and finite but short length (solid line). b) Intensity of the emission of the source 2LS as a function of both the area and the length of the pulse, showing that the Rabi oscillations are quickly suppressed as the length of the pulse is increased. c) Visibility of the Rabi oscillations, as quantified by the normalized difference between the maximum near $A = \pi$ and the minimum near $A = 2\pi$, for the source 2LS (dashed), the target 2LS (ranging between the upper two lines, from solid black to solid blue, covering the entire area shaded in blue) and the photon flux (ranging between the lower two lines, from dashed black to solid red, convering the entire area shaded in red). For the latter two, the gradient indicates the variation of the parameter χ_2. d) Extinction coefficients for the visibility lines showed in panel (c), for the source 2LS (dashed), the target 2LS (blue) and photon flux (red). e,f) Same as in panel (b) but for the target 2LS and the photon flux, respectively; calculated for $\chi_2 = 1/2$. The panels in the bottom row share the same color encoding, and therefore can be compared directly.

finding the extinction coefficient as a function of the χ_2 parameter; showing that the visibility in the oscillations for the target 2LS and the photon flux is optimized in the limit $\chi_2 \to 1$.

4. Time-Integrated Emission Spectra

Beyond the intensity of the light emitted by the 2LS, we now consider the spectral structure of the emission. The time-integrated emission spectra of the various objects in our quantum system are obtained through the calculations of the first-order correlation function $G_c^{(1)}(t,\tau) = \langle c^\dagger(t+\tau)c(t)\rangle$, where $c = \{\sigma, \xi, J_\phi\}$, and then computing the Fourier transform with respect to the delays τ and integrating over the evolution times t; namely

$$S(\omega) = \mathrm{Re}\left[\int_{-\infty}^{\infty} dt \int_{-\infty}^{\infty} d\tau\, G_c^{(1)}(t,\tau) e^{-i\omega\tau}\right] \tag{11}$$

Although the time-integrated emission spectrum of a 2LS driven with pulses of classical light has been already worked out theoretically[28–30] and observed,[59–61] here we reproduce it in **Figure** 3a so that we can compare it with the spectra of the target 2LS and the photon flux. In particular, we observe that the central frequency remains dominant for all pulse areas, along with the lateral peaks arising for $2n\pi$ pulses as a consequence of the dynamic state dressing.[29–31] Figure 3d shows cuts of the density plot for pulse areas $A = \pi$ (solid blue), 2π (solid red), 3π (dashed light blue), and 4π (dot-dashed light red), evidencing the birth, growth and separation of the side peaks as the intensity of the laser increases.

The emission spectra of the target 2LS (which is driven with pulses of quantum rather than classical light) is shown in Figure 3b, where it appears to be given by a single line of oscillating intensity. However, a closer look in logarithmic scale, shown in Figure 3e, reveals that the dynamic dressing of the states of the source 2LS is also imprinted onto the spectrum of the target 2LS. However, in this case, the side bands are much less prominent. Notably, we find that the emission line of the source 2LS, shown as a dotted grey line, is broader than the lines of the target 2LS. As previously observed with quantum excitation in the continuous regime,[62,63] the target 2LS effectively behaves as a filter (of linewidth γ_ξ) of the emission of the source 2LS, thus trimming the fat tails of the Lorentzian profile of the latter. As a consequence, the emission line of the target 2LS is narrower than its natural linewidth γ_ξ and its profile is given by a Student-t distribution of second order.[62] Therefore, we find that the pulsed quantum cascaded excitation also induces a spectral line narrowing in the target 2LS.

Finally, the emission spectrum of the photon flux, shown in Figure 3c, closely resembles its counterpart for the source 2LS.

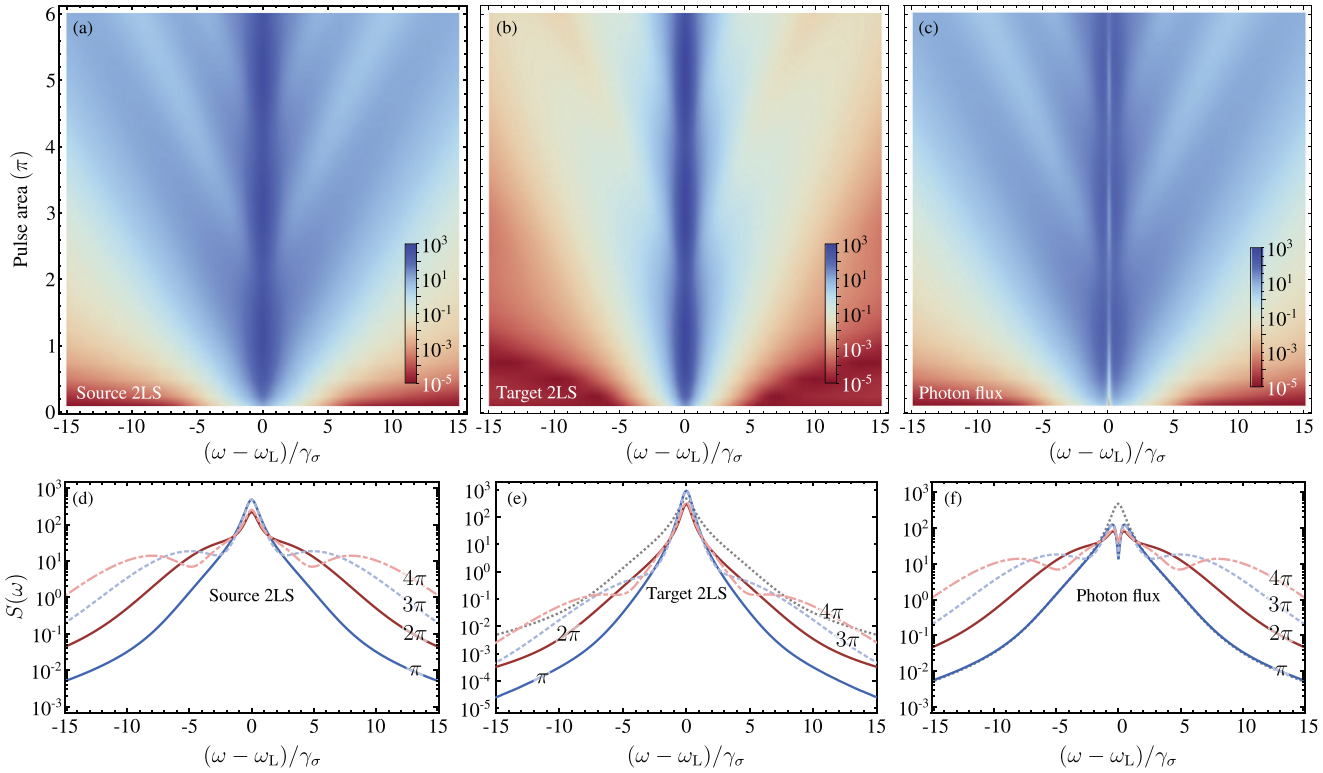

Figure 3. Emission spectra of dynamic Resonance Fluorescence. a–c) Photoluminescence as a function of the area of the pulse, for the source 2LS, target 2LS and the photon flux, respectively. The variation in the intensity of the emission as the pulse area increases is an echo of the Rabi oscillations undergone by the 2LS. d–f) Cuts of the spectra for π- (solid blue), 2π- (solid red), 3π- (dashed light blue) and 4π-pulses (dot-dashed light red). In panels (e) and (f) the dotted gray line corresponds to the PL of the source 2LS for a π-pulse, showing the line narrowing of the target 2LS. The figures are obtained for pulses at resonance to the 2LSs, and setting $\mathcal{W}\gamma_\sigma = 1$ and $\chi_2 = 1/2$. The three upper panels can be compared directly, as they share the same color scaling.

However, we see that exactly at the resonant frequency of the emitters there is a dip in the intensity of the emission: these are the photons that, instead of being observed through the photon flux, are observed directly from the target 2LS. However, the side peaks appear more prominently because, for the photon flux, the maximum of the central peak is reduced. The cuts of the density plot are shown in panel (f) and show that the photon flux does not have any line narrowing (cf. the dotted grey line, corresponding to the PL of the source 2LS for π-pulse excitation), and that the absolute intensity of the side peaks is maintained, which remain as intense as in the figures for the source 2LS.

5. Time-Dependent Occupation

The population of the source 2LS can be described qualitatively as follows: odd-π pulses leave the 2LS in its excited state, followed by the exponential decay associated with the spontaneous emission from the 2LS. Conversely, even-π pulses (almost) leave the 2LS in its ground state. However, the latter statement (without the "almost") is only true in the limit of vanishingly short pulses. Beyond that limit, the 2LS is left in a superposition of its excited and ground states. Therefore, for even-π pulses of finite length, one also observes an exponential decay in the occupation of the 2LS after it has interacted with the whole pulse.

The population of the source 2LS (dashed grey), the target 2LS (dot-dashed blue) and the photon flux (solid red) are shown in **Figure 4** for four pulse areas. On top of the figure there is a sketch of the Gaussian laser pulse exciting the source 2LS. In general, as we found in the previous section, the figures for the photon flux follow closely the behaviour of the source 2LS. However, there are notable differences. First, the curves for the photon flux are less intense, because part of the energy from the source 2LS goes to the target 2LS. Second, the populations for the photon flux display a small, broad peak beyond the main features of the populations. Namely, after the pulse is absorbed, the population does not decrease monotonously. Instead, we see a dip in the occupation (indicated by the arrows), followed by a second peak a few lifetimes later. Although this feature is more prominent for odd-π pulses, it is observed for all pulse areas, even for long pulses (cf. the Supporting Information for an analysis of the effect of the length of the pulse and the coupling parameter χ_2 on the occupations). Formally, the appearance of the delayed peak is a consequence of the interference between the emission from the source and from the target 2LSs, which becomes evident when computing the population of the photon flux, namely $\mathrm{Tr}\{\rho(t)J_\phi^\dagger J_\phi\}$, with J_ϕ the operator in Equation (6). On the other hand, the population of the target 2LS has a less intense profile, which grows and decays smoothly, and extends further in time. Here we no longer see the rapid oscillations induced by the laser pulse, which allows the

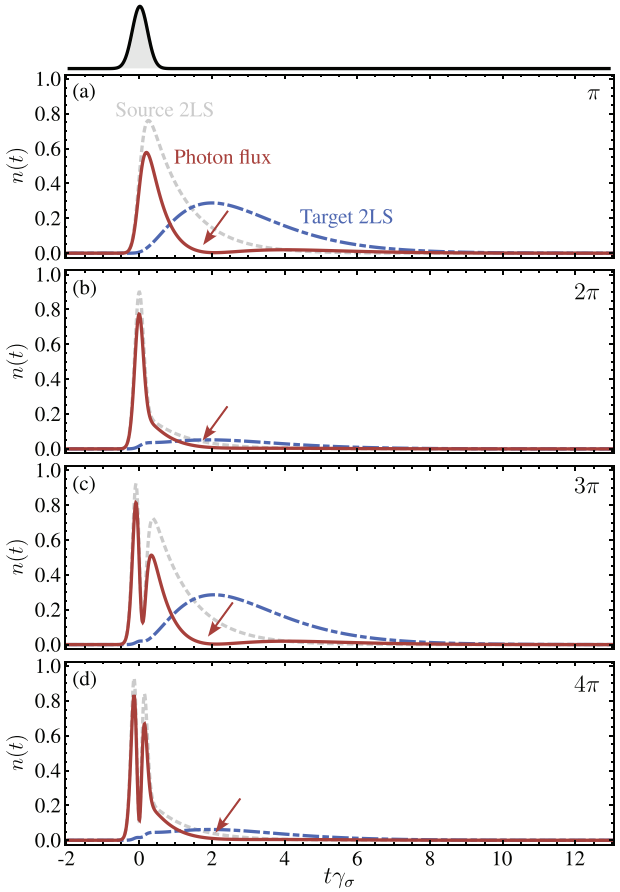

Figure 4. Time-dependent occupation of the pulsed emitters. Comparison between the averaged time-dependent population of the source 2LS (dashed gray), the photon flux (solid red) and the target 2LS (dot-dashed blue), for various pulse areas (noted on the top right corner of each panel). All the panels are obtained with a pulse of length $\mathcal{W}\gamma_\sigma = 1/2$ (which for reference is sketeched at the top of the figure) and letting $\chi_2 = 1/2$. The underlying quantum interference taking place in the field of the photon flux is particularly noticeable in panels (a) and (c), where a dip in the occupation can be distinguished at $t\gamma_\sigma \approx 2$. In all the panels, the origin of time is set by the position of the maximum of the classical pulse.

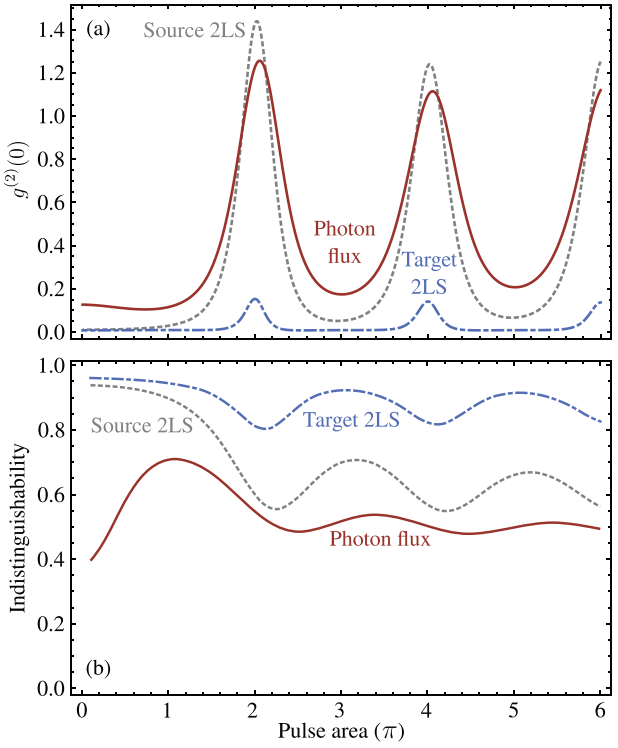

Figure 5. Second-order correlation functions of the emitted photons. a) Zero-delay $g^{(2)}(0)$ and b) Photon indistinguishability, as captured by the visibility of the dip in a HOM interference. Here, we show the information for the source 2LS (dotted gray), the target 2LS (dot-dashed blue) and the photon flux (solid red). In both cases, the figures are obtained with a pulse of $\mathcal{W}\gamma_\sigma = 0.25$ and letting $\chi_2 = 1/2$.

photons to be, on average, further apart from each other than in the field of the source 2LS or of the photon flux. In the next section, we will explore in detail what this implies in terms of the photon antibunching and indistinguishability of the emission.

6. Second-Order Correlations

6.1. Enhancement of the Antibunching

We now turn to two-photon observables and delve into the temporal structure of the light. Specifically, we consider the second-order coherence function $g^{(2)}(0)$ of the emission. **Figure** 5a shows the correlation function of the source 2LS (dashed grey), the photon flux (solid red) and the target 2LS (dot-dashed blue) as a function of the area of the pulse.

The figures show the ratio of the correlations between photons emitted from a single pulse and the correlations between photons emitted from different pulses. Namely, the normalization commonly done in experiments with pulsed excitation. For the source 2LS, shown as gray dashed line in Figure 5a, we find a well-known result: the correlations are bunched for even-π pulses and antibunched for odd-π pulses. This is because for even-π pulses, the probability to measure two photons P_2 is larger than the probability to measure only one photon P_1,[60] while the overall intensity of the emission is at its minimum [cf. Figure 2a]. The combination of these two facts yields bunching among the emitted photons. For odd-π pulses the reverse is true: $P_1 > P_2$, the intensity of the emission is at its maximum, and as a consequence we observe antibunching. In the intermediate pulse areas, the system undergoes a smooth transition between these two limits. Considering now the photon flux of the system, shown in solid red, we find a nice match with the recent experimental observation,[36] confirming that the output field measured in the experiment was actually the photon flux of the system, and not only the luminescence from the target 2LS. Thus, the photons of the photon flux are always less antibunched than those of the source 2LS, except at a region in the vicinity of 2π (from our theoretical calculation, we find that this is true in the vicinity of $2n\pi$), where the relation is reversed. This is because the incoming temporally separated two-photon components are partially changed to one-photon components in the detected output field, leading to lower $g^{(2)}(0)$ values in the photon flux.[36] However, at such pulse areas, the photons are bunched, so there is no enhancement of the single-photon emission. However, turning to the emission from the target 2LS, we

find that their photon are always more antibunched than those emitted by the source 2LS. This observation is in agreement with previous theoretical predictions made on cascaded structures excited with cw-excitation.[20] Notably, even for $2n\pi$ pulses, where the photons of both the source 2LS and the photon flux are bunched, the emission from the target 2LS remains antibunched. Thus, here we provide evidence that the quantum cascaded excitation is a mechanism to improve the antibunching in pulsed systems. (In the Supporting Information we show how these correlations vary depending on the length of the classical pulse, and that our results hold even with ultra-short pulses, used in state-of-the-art setups to extract single photons.[64,65]) Namely, as the pulses become broader, the maxima of the correlations, which still occur for pulses of (approximately) even-π areas, remain antibunched, i.e., below 1. Thus, even if the emission for, e.g., 2π-pulses is expected to be a bunched pair of photons, this is only true in the limit of small pulse lengths. When the latter condition is not fulfilled, the photons pairs are less antibunched than those emitted from, e.g., π-pulses, but remain antibunched nonetheless. In the limit of very long pulses, where the excitation profile becomes essentially flat, we recover the results of cw-excitation; namely, perfect antibunching in the source 2LS, target 2LS and the photon flux. Moreover, in the same way in which the maxima and minima of the Rabi oscillations drift away from integer-π-pulses, as the length of the pulses increases, the maxima of correlations also drift away from the even-π-pulses; which is specially visible for the case of the photon flux (cf. the Supporting Information).

6.2. Enhancement of the Indistinguishability

Once we have established that the quantum excitation yields an enhancement in the antibunching of the emission, we address another important characteristic of sources of single photons, namely their indistinguishability. Such a property is measured with a Hong-Ou-Mandel (HOM) interferometer,[66] whereby the visibility of the interference is directly related to the indistinguishability of the input states,[67–69] even for imperfect sources of single photons.[70] Figure 5b shows the indistinguishability of the photons emitted by the source 2LS (dashed gray), the target 2LS (dot-dashed blue) and the photon flux (solid red) as a function of the area of the pulse. Comparing the values obtained for π-pulses, we find a very good agreement with the recent experimental observations:[36] the source 2LS yields photons with a $\approx 91\%$ indistinguishability, while for the photon flux this value decreases to $\approx 75\%$. Such a drop of the indistinguishability is clear considering that the observed field is made of the quantum superposition of two fields: one from each 2LS. Such a superposition, together with the quantum interference that inherently takes place in the dynamics of the photon flux, is what makes the photons more distinguishable. Conversely, considering the photons emitted by the target 2LS, we find that they are more indistinguishable than those emitted by the source 2LS: for π-pulses, we find a $\approx 95\%$ indistinguishability. Further, although the photons from the target 2LS are always more indistinguishable than the ones from the source 2LS, the enhancement is more prominent near even-π pulses, where the target 2LS provides photons up to 45% more indistinguishable than the source 2LS. Therefore, quantum excitation provides an enhancement of both the antibunching and the indistinguishability of the emission.

6.3. Signatures of Stimulated Emission

In the previous two subsections, we have considered the correlations between photons in different pulses. However, the question about the correlations between photons within a single pulse remains open. Here we provide an answer, and we will begin with the two-particle correlation function $G_c^{(2)}(t_1,t_2) = \langle c^\dagger(t_2)c^\dagger(t_1)c(t_1)c(t_2)\rangle$ with $c = \{\sigma, \xi, J_\phi\}$ for the source 2LS, the target 2LS and the photon flux, respectively. Such a function captures the correlations between photons (not necessarily consecutive) emitted at times t_1 and t_2, respectively. Thus, we compute a two-photon correlation map that, instead of their frequencies,[17–19,71–74] takes into account their emission times. **Figure 6** shows the delayed correlations of photon pairs emitted from the source 2LS, the target 2LS and the photon flux. Although the correlation map from the target 2LS seems to be a copy from the correlations for the source 2LS, the time scales in the two figures are different. The correlation in the target 2LS decays almost twice as slowly as its counterpart for the source 2LS. Such an observation is also in agreement with the fact that the emission from the target 2LS is also more spread in time, as we showed in Figure 4 and discussed in the previous sections. On the other hand, the correlations from the photon flux are qualitatively different from those of the bare 2LSs. In fact, while the correlations $G_\sigma^{(2)}(t,t)$ and $G_\xi^{(2)}(t,t)$ are exactly zero at all times, because the operators σ and ξ are nilpotent (i.e., $\sigma^2 = 0$), for the photon flux we find $G_\phi^{(2)}(t,t) = 4\chi_1\chi_2\gamma_\sigma\gamma_\xi\langle\sigma^\dagger\sigma\xi^\dagger\xi\rangle(t)$, which can be nonzero, indicating the joint occupation of the two 2LS. Indeed, instead of the fairly straight correlation lines at either $t_1\gamma_\sigma \approx 0$ or $t_2\gamma_\sigma \approx 0$, we observe the appearance of correlations along the diagonal of the figure, that is, for $t_1 = t_2$. These correlations imply that there are pairs of photons emitted simultaneously, which is a signature of *stimulated emission* between a single (excited) emitter and a single photon.[75] It is important to keep in mind that the diagonal line appearing on Figure 6c, which indicates emission at zero delay, truly indicates simultaneous emission, and it is not equivalent to the results shown in Figure 4, where the zero delay refers to emission within a single pulse. Furthermore, note that the results shown in Figure 6 correspond to an excitation pulse of area π, which usually is regarded as a single photon excitation pulse. Thus, our results also reveal the Poissonian character of the laser pulse: sometimes, a photon from the pulse excites the 2LS. Later, a subsequent photon from the same pulse, which is only there because of the fluctuations of the photon number in the coherent state of the laser, reaches the now-excited-2LS, which then leads to the generation of two photons in the photon flux of the system. These same-time correlations have a dynamics similar to the one of the occupations, showing traces of the Rabi oscillations as a function of the area of the pulse (cf. the Supporting Information for the details). However, all of them decay with an exponent $\gamma_d = 2\gamma_\sigma$, which indicates that the lifetime of these correlations is half of the lifetime of the spontaneous emission, i.e., $\tau_d = \tau_\sigma/2$, in agreement with the recent experimental observations.[36]

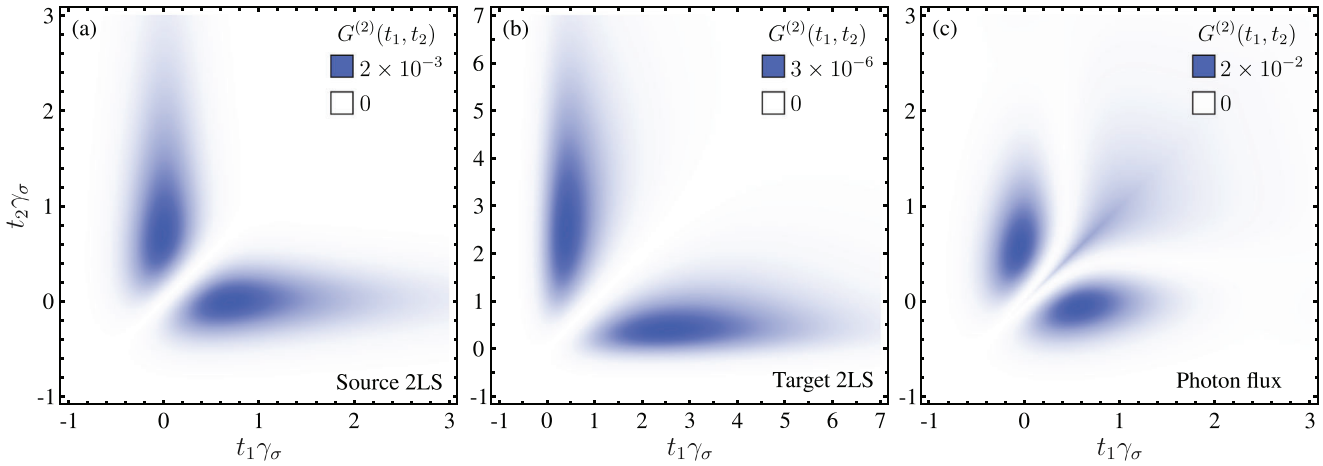

Figure 6. Time-delayed second-order coherence function $G^{(2)}(t_1, t_2)$. a) Correlation function for the source 2LS, displaying correlations between photons emitted in the close vicinity of the maximum of the excitation pulse. b) The target 2LS inherits the shape of its correlation from the source 2LS, but although they have the same decay rate γ_σ, the correlations of the target 2LS spread further in time and are attenuated by over three orders of magnitude. c) The photon flux also has the lobes around the maximum of the excitation pulse, but displays correlations on the diagonal of the figure, which correspond to photons emitted simultaneously ($t_1 = t_2$) and beyond the lifetime of the 2LS. The figure corresponds to excitation with a π-pulse of length $\mathcal{W}\gamma_\sigma = 1$. In all the panels, the origin of time is set by the position of the maximum of the classical pulse.

Now that we have identified the quantum correlations associated with stimulated emission, we can quantify them through their normalized version, shown in **Figure 7**. The first notable observation from this figure is that the process of stimulated emission does not take place only at large pulse areas. In fact, the photon flux always displays such a process, and it is precisely when the classical pulses are weak that the correlations are the strongest! In fact, in the same way in which it was found in Resonance Fluorescence upon frequency-filtering, the strongest correlations appear in the regions where the emission is the scarcest.[17,18] Namely, in a process akin to distillation, the strong correlations are what is left once the other processes are not present. The second observation from this figure is the fact that the bunching in the zero-delay correlations of the photon flux coincides with the appearance of the second excitation peak in the time-dependent occupation, which appears after the dip due to the quantum interference of the fields, as we showed in Figure 4. These peaks, that extend for over two lifetimes, and for even-π pulses are even longer, remain bunched throughout, and therefore constitute another mechanism to extract highly correlated photons by filtering the emission in time.

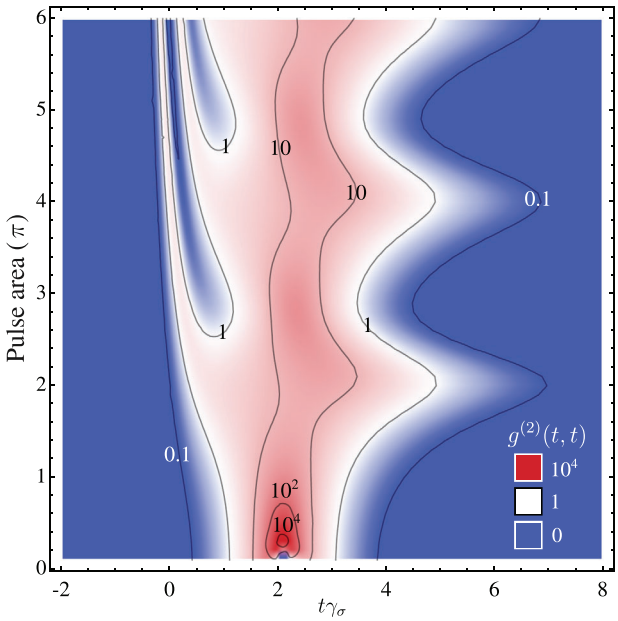

Figure 7. Normalized time-dependent correlation function of the photons within a single pulse, $g^{(2)}(t, t)$. While the correlations of the source and target 2LS are exactly zero for all t, the photon flux displays bunching lasting for over two lifetimes. The figure was obtained for a pulse of width $\mathcal{W}\gamma_\sigma = 1$ and letting $\chi_2 = 1/2$. The origin of time is set by the position of the maximum of the classical pulse.

7. Discussion and Conclusion

Based on recent experimental results,[36] we have presented a thorough theoretical description of the dynamics of a quantum system under pulsed quantum excitation. In our description, we have used the most fundamental, and phenomenologically rich, quantum system available, a 2LS, both as the source and the optical target of the quantum light. Notably, our model does not require the addition of any dephasing mechanisms to fully reproduce the experimental observation of our system.[36] Thus, this indicates that for high-quality semiconductor quantum dots, the naturally occurring dephasing processes do not spoil our observations. First, we showed that the expected Rabi oscillations in the total emission, predicted from the pulse area theorem, are visible only when the length of the driving pulse is significantly shorter than the lifetime of the 2LS. When such a condition is not met, the visibility of the oscillations starts to decrease down to the point in which one cannot longer speak of oscillations, as the intensity of the emission increases monotonically. Furthermore, we found that the maxima and minima of the Rabi oscillations are given exactly by even- and odd-π-pulses, respectively. How-

ever, such an expectation is only met in the limit of ultra-short pulses, and the position of the maxima and minima drift away as the length of the pulse increases. Thus, we showed that, together with dissipation and coupling to phonon fields, the length of the pulse is yet another mechanism that induces a shift in the position of the maxima and minima of the Rabi oscillations.

Continuing with the single-particle observables, we found that both the time-integrated spectrum and the occupation of the source 2LS are inherited closely by the photon flux. On the other hand, although the emission spectra of the target 2LS appears to be a single line, the dynamical dressing of the source 2LS is also inherited here, but with a much smaller intensity. However, it is noteworthy that the linewidth of the target 2LS, driven with quantum light, is narrower than the linewidth of the source 2LS. In fact, a closer inspection of the occupation of the target 2LS and the photon flux, revealed that a considerable part of the light is emitted well beyond the limits of one lifetime of the 2LS.

The relevance of such a delayed emission is unveiled when considering the two-particle observables, namely the second-order coherence function. The photon flux displays strong bunching in its zero-delay correlation, which is an indication of stimulated emission from the system. Such an observation is supported by two facts: first they are not present in the figures of the source nor the target 2LSs, and second the lifetime of these correlations is exactly half the lifetime of the spontaneously emitted photons. Finally, we also found that the light emitted from the target 2LS is always more antibunched and more indistinguishable than the emission from the source 2LS. Thus, we demonstrated that pulsed quantum excitation can be used as a mechanism to produce subnatural linewidth antibunched light, as shown in Refs. [20, 62] for continuous coherent driving.

The approach used here, namely, the consideration of pulsed rather than continuous excitation, makes our findings accessible to experimental groups with state-of-the-art setups. Thus, we believe that our results can be used as a guideline to the exploration of quantum phenomena arising in condensed matter physics, and to work towards the resolution of both fundamental and practical questions. For instance, the photon flux emission is a natural resource that can be used to exploit quantum interferences and develop, e.g., mechanisms akin to homodyne detection, or two-photon interference protocols, and even extract varying types of photon correlations by selecting the frequency range of their emission.[35] Alternatively, starting from the results from the target 2LS, we can envisage a mechanism to generate more antibunched and more indistinguishable photons emitted with a narrower line. Notably, our results are also valid in the regime of operation of modern sources of single photons,[64,65] namely when the length of the laser pulse is about two orders of magnitude shorter than the lifetime of the emitter (cf. Figure S4, Supporting Information). In fact, such a mechanism could be constructed in a cascaded scheme, and then one should consider whether the antibunching, the indistinguishability and the line narrowing of the emission can be further improved as the number of steps in the cascade increases. Furthermore, a natural continuation for this work would be to include chirping[76] into the description of the pulse, or to consider other types of quantum light as the source of excitation. For instance, photon streams with a varying coherence function (which could be used as a spectroscopy tool) or other types of quantum correlations, including entanglement.

Supporting Information

Supporting Information is available from the Wiley Online Library or from the author.

Acknowledgements

The author thanks Lena M. Hansen and Í. Arrazola for interesting discussions and feedback on early versions of the manuscript. This research was funded in whole by the Polish National Science Center (NCN) "Sonatina" project CARAMEL with number 2021/40/C/ST2/00155. For the purpose of Open Access, the author has applied CC-BY public copyright licence to any Author Accepted Manuscript (AAM) version arising from this submission.

Conflict of Interest

The authors declare no conflict of interest.

Data Availability Statement

The data that support the findings of this study are available from the corresponding author upon reasonable request.

Keywords

excitation with quantum light, pulsed excitation, resonance fluorescence, single-photon sources, stimulated emission

Received: June 3, 2025
Revised: September 16, 2025
Published online:

[1] H. J. Carmichael, D. F. Walls, *J. Phys. B.: At. Mol. Phys.* **1976**, *9*, 1199.
[2] B. Yurke, *Phys. Rev. A* **1984**, *29*, 408(R).
[3] M. J. Collett, C. W. Gardiner, *Phys. Rev. A* **1984**, *30*, 1386.
[4] G. Rempe, R. J. Thompson, R. J. Brecha, W. D. Lee, H. J. Kimble, *Phys. Rev. Lett.* **1991**, *67*, 1727.
[5] E. S. Polzik, J. Carri, H. J. Kimble, *Phys. Rev. Lett.* **1992**, *68*, 3020.
[6] Z. Y. Ou, S. F. Pereira, H. J. Kimble, K. C. Peng, *Phys. Rev. Lett.* **1992**, *68*, 3663.
[7] C. W. Gardiner, *Phys. Rev. Lett.* **1993**, *70*, 2269.
[8] H. J. Carmichael, *Phys. Rev. Lett.* **1993**, *70*, 2273.
[9] C. A. Downing, J. C. López Carreño, F. P. Laussy, E. del Valle, A. I. Fernández-Domínguez, *Phys. Rev. Lett.* **2019**, *122*, 057401.
[10] K. Sun, W. Yi, *Phys. Rev. A* **2023**, *108*, 013302.
[11] B. Tissot, G. Burkard, *Phys. Rev. Research* **2024**, *6*, 013150.
[12] Y. Xiang, S. Cheng, Q. Gong, Z. Ficek, Q. He, *PRX Quantum* **2022**, *3*, 030102.
[13] S. Ghosh, A. Opala, M. Matuszewski, T. Paterek, T. C. H. Liew, *npj Quantum Inf* **2019**, *5*, 35.
[14] S. Ghosh, A. Opala, M. Matuszewski, T. Paterek, T. C. H. Liew, *IEEE Trans. Neural Netw. Learning Syst.* **2020**, *32*, 3148.
[15] J. Dudas, B. Carles, E. Plouet, F. A. Mizrahi, J. Grollier, D. Marković, *npj Quantum Inf* **2023**, *9*, 64.
[16] B. R. Mollow, *Phys. Rev.* **1969**, *188*, 1969.
[17] J. C. López Carreño, E. del Valle, F. P. Laussy, *Laser Photon. Rev.* **2017**, *11*, 1700090.
[18] A. González-Tudela, F. P. Laussy, C. Tejedor, M. J. Hartmann, E. del Valle, *New J. Phys.* **2013**, *15*, 033036.

[19] M. Peiris, B. Petrak, K. Konthasinghe, Y. Yu, Z. C. Niu, A. Muller, *Phys. Rev. B* **2015**, *91*, 195125.
[20] J. C. López Carreño, C. Sánchez Muñoz, E. del Valle, F. P. Laussy, *Phys. Rev. A* **2016**, *94*, 063826.
[21] J. C. López Carreño, F. P. Laussy, *Phys. Rev. A* **2016**, *94*, 063825.
[22] J. C. López Carreño, C. Sánchez Muñoz, D. Sanvitto, E. del Valle, F. P. Laussy, *Phys. Rev. Lett.* **2015**, *115*, 196402.
[23] P. A. Rodgers, S. Swain, *Optics Commun.* **1991**, *81*, 291.
[24] K. Rzążewski, M Florjańczyk, *J. Phys. B: At. Mol. Phys.* **1984**, *17*, L509.
[25] R. Buffa, S. Cavalieri, L. Fini, M. Matera, *J. Phys. B: At. Mol. Opt. Phys.* **1988**, *21*, 239.
[26] M. Lewenstein, J. Zakrzewski, K. Rzążewski, *J. Opt. Soc. Am. B* **1986**, *3*, 22.
[27] Y. He, Y.-M. He, J. Liu, Y.-J. Wei, H. Y. Ramírez, M. Atatüre, C. Schneider, M. Kamp, S. Höfling, C.-Y. Lu, J.-W. Pan, *Phys. Rev. Lett.* **2015**, *114*, 097402.
[28] M. Florjańczyk, K. Rzążewski, J. Zakrzewski, *Phys. Rev. A* **1985**, *31*, 1558.
[29] A. Moelbjerg, P. Kaer, M. Lorke, J. Mørk, *Phys. Rev. Lett.* **2012**, *108*, 017401.
[30] C. Gustin, R. Manson, S. Hughes, *Opt. Lett., OL* **2018**, *43*, 779.
[31] K. Boos, S. K. Kim, T. Bracht, F. Sbresny, J. M. Kaspari, M. Cygorek, H. Riedl, F. W. Bopp, W. Rauhaus, C. Calcagno, J. J. Finley, D. E. Reiter, K. Müller, *Phys. Rev. Lett.* **2024**, *132*, 053602.
[32] X. Ruan, Jia-H. Wang, D. He, P. Song, S. Li, Q. Zhao, L. M. Kuang, J.-S. Tsai, C.-L. Zou, J. Zhang, D. Zheng, O. V. Astafiev, Yu-x. Liu, Z. Peng, *Phys. Rev. Res.* **2024**, *6*, 033064.
[33] S. Liu, C. Gustin, H. Liu, X. Li, Y. Yu, H. Ni, Z. Niu, S. Hughes, X. Wang, J. Liu, *Nat. Photon.* **2024**, *18*, 318.
[34] K. Konthasinghe, M. Peiris, B. Petrak, Y. Yu, Z. C. Niu, A. Muller, *Opt. Lett.* **2015**, *40*, 1846.
[35] S. Bermúdez Feijóo, E. Zubizarreta Casalengua, K. Müller, K. D. Jöns, *Phys. Rev. Research* **2025**, *7*, 033296.
[36] L. M. Hansen, F. Giorgino, L. Jehle, L. Carosini, J. C. López Carreño, I. Arrazola, P. Walther, J. C. Loredo, *arXiv:2407.20936* (**2024**).
[37] A. L. Grimsmo, *Phys. Rev. Lett.* **2015**, *115*, 060402.
[38] S. J. Whalen, A. L. Grimsmo, H. J. Carmichael, *Quantum Sci. Technol.* **2017**, *2*, 044008.
[39] H.-P. Breuer, E.-M. Laine, J. Piilo, B. Vacchini, *Rev. Mod. Phys.* **2016**, *88*, 021002.
[40] I. De Vega, D. Alonso, *Rev. Mod. Phys.* **2017**, *89*, 015001.
[41] K. Sinha, P. Meystre, E. A. Goldschmidt, F. K. Fatemi, S. L. Rolston, P. Solano, *Phys. Rev. Lett.* **2020**, *124*, 043603.
[42] R. J. Cook, P. W. Milonni, *Phys. Rev. A* **1987**, *35*, 5081.
[43] U. Dorner, P. Zoller, *Phys. Rev. A* **2002**, *66*, 023816.
[44] T. Tufarelli, F. Ciccarello, M. S. Kim, *Phys. Rev. A* **2013**, *87*, 013820.
[45] A. Carmele, J. Kabuss, F. Schulze, S. Reitzenstein, A. Knorr, *Phys. Rev. Lett.* **2013**, *110*, 013601.
[46] P.-O. Guimond, A. Roulet, H. N. Le, V. Scarani, *Phys. Rev. A* **2016**, *93*, 023808.
[47] C. W. Hsu, B. Zhen, A. D. Stone, J. D. Joannopoulos, M. Soljačić, *Nat. Rev. Mater.* **2016**, *1*, 16048.
[48] P. T. Fong, C. K. Law, *Phys. Rev. A* **2017**, *96*, 023842.
[49] P. Facchi, D. Lonigro, S. Pascazio, F. V. Pepe, D. Pomarico, *Phys. Rev. A* **2019**, *100*, 023834.
[50] C. Gonzalez-Ballestero, F. J. García-Vidal, E. Moreno, *New J. Phys.* **2013**, *15*, 073015.
[51] H. Pichler, P. Zoller, *Phys. Rev. Lett.* **2016**, *116*, 093601.
[52] H. Qiu, Y. You, Xi-H. Guan, Xiao-J. Du, J. He, Zhong-J. Yang, *Phys. Rev. B* **2024**, *110*, 075432.
[53] J. Dalibard, Y. Castin, K. Mølmer, *Phys. Rev. Lett.* **1992**, *68*, 580.
[54] J. C. López Carreño, S. Bermudez Feijoo, M. Stobińska, *npj Nanophoton.* **2024**, *1*, 3.
[55] A. H. Kiilerich, K. Mølmer, *Phys. Rev. Lett.* **2019**, *123*, 123604.
[56] A. H. Kiilerich, K. Mølmer, *Phys. Rev. A* **2020**, *102*, 023717.
[57] L. Allen, J. H. Eberly, *Optical Resonance and Two-Level Atoms*, (Dover1987).
[58] D. A. Steck, *Quantum and Atom Optics* available online at http://steck.us/teaching (revision 0.16.2, November 2024) ed., **2024**.
[59] K. A. Fischer, K. Müller, A. Rundquist, T. Sarmiento, A. Y. Piggott, Y. A. Kelaita, C. Dory, K. G. Lagoudakis, K. Müller, J. Vučković, *Nat. Photon.* **2016**, *10*, 163.
[60] K. A. Fischer, L. Hanschke, J. Wierzbowski, T. Simmet, C. Dory, J. J. Finley, J. Vučković, K. Müller, *Nat. Phys.* **2017**, *4*, 649.
[61] L. Masters, Xin-X. Hu, M. Cordier, G. Maron, L. Pache, A. Rauschenbeutel, M. Schemmer, J. Volz, *Nat. Photon.* **2023**, *17*, 972.
[62] J. C. López Carreño, E. Zubizarreta Casalengua, F. P. Laussy, E. del Valle, *Quantum Sci. Technol.* **2018**, *3*, 045001.
[63] J. C. López Carreño, E. Zubizarreta Casalengua, F. P. Laussy, E. del Valle, *J. Phys. B: At. Mol. Opt. Phys.* **2019**, *52*, 035504.
[64] N. Somaschi, V. Giesz, L. De Santis, J. C. Loredo, M. P. Almeida, G. Hornecker, S. L. Portalupi, T. Grange, C. Antón, J. Demory, C. Gómez, I. Sagnes, N. D. Lanzillotti-Kimura, A. Lemaître, A. Auffeves, A. G. White, L. Lanco, P. Senellart, *Nat. Photon.* **2016**, *10*, 340.
[65] N. Tomm, A. Javadi, N. O. Antoniadis, D. Najer, M. C. Löbl, A. R. Korsch, R. Schott, S. R. Valentin, A. D. Wieck, A. Ludwig, R. J. Warburton, *Nat. Nanotechnol.* **2021**, *16*, 399.
[66] C. K. Hong, Z. Y. Ou, L. Mandel, *Phys. Rev. Lett.* **1987**, *59*, 2044.
[67] J. Bylander, I. Robert-Philip, I. Abram, *Eur. Phys. J. D* **2003**, *22*, 295.
[68] T. Legero, T. Wilk, A. Kuhn, G. Rempe, *Appl. Phys. B* **2003**, *77*, 797.
[69] R. Trivedi, K. A. Fischer, J. Vučković, K. Müller, *Adv Quantum Tech* **2020**, *3*, 1900007.
[70] H. Ollivier, S. E. Thomas, S. C. Wein, I. M. De Buy Wenniger, N. Coste, J. C. Loredo, N. Somaschi, A. Harouri, A. Lemaitre, I. Sagnes, L. Lanco, C. Simon, C. Anton, O. Krebs, P. Senellart, *Phys. Rev. Lett.* **2021**, *126*, 063602.
[71] E. del Valle, A. González-Tudela, F. P. Laussy, C. Tejedor, M. J. Hartmann, *Phys. Rev. Lett.* **2012**, *109*, 183601.
[72] B. Piętka, J. Suffczyński, M. Goryca, T. Kazimierczuk, A. Golnik, P. Kossacki, A. Wysmolek, J. A. Gaj, R. Stępniewski, M. Potemski, *Phys. Rev. B* **2013**, *87*, 035310.
[73] B. Silva, C. Sánchez Muñoz, D. Ballarini, A. González-Tudela, M. de Giorgi, G. Gigli, K. West, L. Pfeiffer, E. del Valle, D. Sanvitto, F. P. Laussy, *Sci. Rep.* **2016**, *6*, 37980.
[74] J. C. López Carreño, E. del Valle, F. P. Laussy, *Sci. Rep.* **2018**, *8*, 6975.
[75] E. Rephaeli, S. Fan, *Phys. Rev. Lett.* **2012**, *108*, 143602.
[76] F. Kappe, Y. Karli, G. Wilbur, R. G. Krämer, S. Ghosh, R. Schwarz, M. Kaiser, T. K. Bracht, D. E. Reiter, S. Nolte, K. C. Hall, G. Weihs, V. Remesh, *Adv. Quantum Tech.* **2024**, 2300352.